Molecular Switches

DOI: 10.1002/anie.201001536

A Double-Switching Multistable Fe_4 Grid Complex with Stepwise Spin-Crossover and Redox Transitions**

*Benjamin Schneider, Serhiy Demeshko, Sebastian Dechert, and Franc Meyer**

Dedicated to Professor Peter Paetzold on the occasion of his 75th birthday

One of the requirements for the development of novel materials for high-density information storage is switchability on the molecular level. Such molecular electronics can be realized by different intrinsic properties of the molecule. Spin-crossover (SCO) behavior, where molecular species (mostly iron(II) complexes) switch between high-spin (HS) and low-spin (LS) states, has long been discussed as a promising way of attaining bi- or even multistability.[1] Whilst most SCO systems are mononuclear, in recent years significant progress has also been seen in the field of dinuclear[2] (including pyrazolate bridged[2c–f]) and polynuclear SCO compounds.[3] An interesting class of compounds in this context are grid complexes, which provide a matrix-like array of addressable sites whose size is even smaller than quantum dots.[4] However, the number of grid-type Fe_4 complexes has remained very limited,[5–9] and only very few exhibit SCO bi- or multistability.[5,6,9] The first $[2\times2]$ Fe_4 grid complexes of this type, which were based on pyrimidine-derived compartmental ligand strands, were published by Lehn et al. in 2000 and showed continuous and incomplete spin transition between three magnetic levels.[5] Some cyanide-bridged tetranuclear ferrous squares contain two low-spin and two SCO sites, where the latter show two-step spin conversion depending on the capping ligand.[6] Recently Sato et al. reported an oxo-bridged Fe^{II}_4 cluster that undergoes abrupt thermally induced and complete photoinduced spin transition, which surprisingly occurs on the same side of the ferrous square to give a *cis*-[LS-LS-HS-HS] geometric configuration at low temperatures.[9]

Alternatively, switching in molecular squares may be achieved electrochemically. A tetrairon $[2\times2]$ grid complex has recently been described that features four successive redox processes and forms a stable di-mixed-valence state.[7b] Such systems attract particular interest as potential "quantum cellular automata" (QCA) with four dots located at the vertices of a square. In these QCAs, binary information is encoded in the charge configuration of a molecular cell that is composed of differently charged redox centers, and not in the on/off state of a current switch.[7b,10,11]

Compartmental polypyridyl ligands are the most prominent class of ligand strands to induce the formation of grid-type complexes in a self-assembly process.[12] We have recently developed a rigid pyrazole-bridged binucleating ligand L^- that provides two tridentate terpyridine-like binding pockets and forms very robust and compact grid complexes with various 3d transition metal ions, such as Co^{II}, Mn^{II}, and Cu^{II}.[13] The anionic nature of this scaffold leads to a lower overall charge of the M^{II}_4 square compared to, for example, the pyrimidine-based systems, which we expected to be beneficial for sequential oxidation up to M^{III}_4 species. Herein we present a Fe_4 $[2\times2]$ grid complex of L^- that shows an unprecedented multistability with respect to both spin transitions and redox transformations (Figure 1).

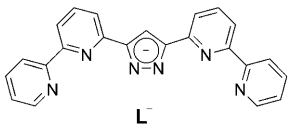

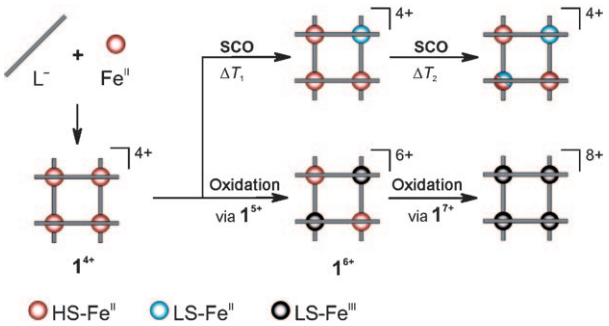

Figure 1. Overview of the chemical and physical transformations of the Fe_4 grid complex.

Treatment of HL with NEt_3 or KO*t*Bu in THF and subsequent reaction with $Fe(BF_4)_2\cdot6H_2O$ in MeCN gives $[Fe_4L_4](BF_4)_4$ (**1**$(BF_4)_4$) in a spontaneous self-assembly process. Its identity was confirmed by ESI mass spectrometry and elemental analysis. Crystals of **1**$(BF_4)_4\cdot4$DMF were obtained by slow diffusion of diethyl ether into a deep red solution of the complex in DMF.

The molecular structure of $\mathbf{1}^{4+}$ in the solid state documents the anticipated formation of the $[2\times2]$ grid complex (Figure 2, left). The four Fe^{II} ions are situated at the corners of a square in a strongly distorted octahedral $\{N_6\}$ ligand

[*] Dipl.-Chem. B. Schneider, Dr. S. Demeshko, Dr. S. Dechert, Prof. Dr. F. Meyer
Institut für Anorganische Chemie
Georg-August-Universität Göttingen
Tammannstrasse 4, 37077 Göttingen (Germany)
Fax: (+49) 551-39-3063
E-mail: franc.meyer@chemie.uni-goettingen.de
Homepage: http://www.meyer.chemie.uni-goettingen.de

[**] Financial support from the DFG (SFB 602, project A16) is gratefully acknowledged.

Supporting information for this article is available on the WWW under http://dx.doi.org/10.1002/anie.201001536.

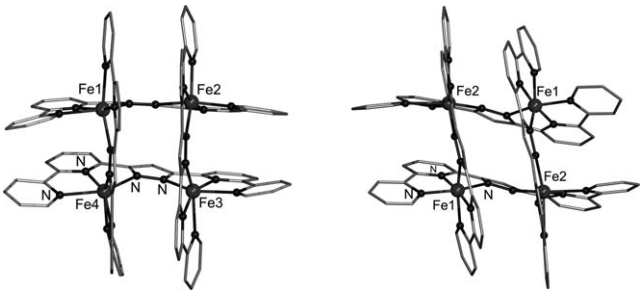

Figure 2. Molecular structure of $\mathbf{1}^{4+}$ (left) and $\mathbf{1}^{6+}$ (right) at 133 K in the solid state. Counterions, solvent molecules, and hydrogen atoms are omitted for clarity.

surrounding that is composed of two orthogonal terpyridine-like subunits from two different ligand strands. Inspection of the Fe–N bond lengths usually allows HS-Fe^{II} and LS-Fe^{II} to be distinguished from another.[14] Thus, at 133 K, three of the ions are in the HS state (mean bond length d [Å]: Fe1–N 2.17, Fe3–N 2.18, Fe4–N 2.19) and one in the LS state (d(Fe2–N) = 1.99 Å). The HS state is accompanied by a more pronounced distortion of the octahedral structure: the average N-Fe-N angles deviate from those of the ideal octahedron by 14% in the HS situation, in contrast to only 9% in the LS case. X-ray analysis at 233 K indicates a LS–HS transition for Fe2. The average Fe–N bonds for Fe2 are stretched by $\Delta d = 0.17$ Å to $d = 2.16$ Å in the $(\text{HS-Fe}^{II})_4$ state. The aromatic subunits of the ligand strands in $\mathbf{1}^{4+}$ are not arranged in a strictly coplanar manner, but are tilted by up to 16.5°.

The temperature dependence of the product $\chi_M T$ for $\mathbf{1}^{4+}$ in the range 300–5 K can be subdivided into three sections (Figure 3). Cooling from 300 to 140 K causes a decrease of $\chi_M T$ ($14.3 \rightarrow 10.7$ $cm^3 K mol^{-1}$) that corresponds to a thermal SCO of one of the four Fe^{II} centers ($S = 2 \rightarrow S = 0$). The $\chi_M T$ values fit the expected values for uncoupled spins well. Below this temperature, $\chi_M T$ further decreases to reach a plateau at 9.0 $cm^3 K mol^{-1}$. This section can be ascribed to the partial SCO of a second Fe^{II} center. The steep decrease of the curve to 4.0 $cm^3 K mol^{-1}$ upon further cooling can be explained by zero-field splitting (in both forms, 2HS–2LS and 3HS–LS) and

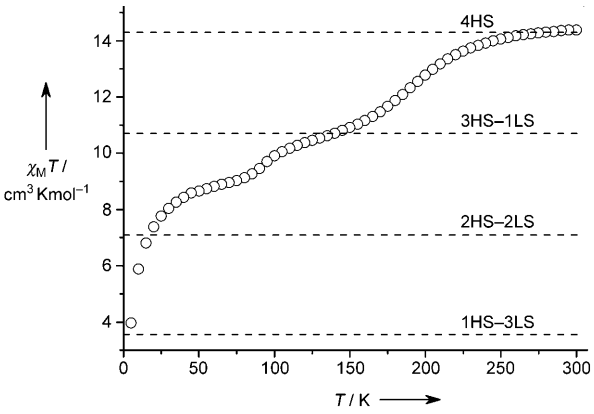

Figure 3. $\chi_M T$ versus T plot of $\mathbf{1}^{4+}$. Spin-only values for the different spin-state combinations in the grid complex are represented by the dotted lines.

antiferromagnetic coupling ($J = -0.4$ cm^{-1}) between the residual HS-Fe^{II} in the [HS-HS-HS-LS] form (see the Supporting Information, Figure S1).

^{57}Fe Mössbauer spectra of $\mathbf{1}(BF_4)_4 \cdot 4\,DMF$ were recorded at selected temperatures between 295 K and 5 K. At room temperature, one quadrupole doublet with parameters typical for HS-Fe^{II} is observed ($\delta = 0.92$ $mm\,s^{-1}$, $\Delta E_Q = 2.02$ $mm\,s^{-1}$; green subspectrum in Figure 4). This, in accordance with

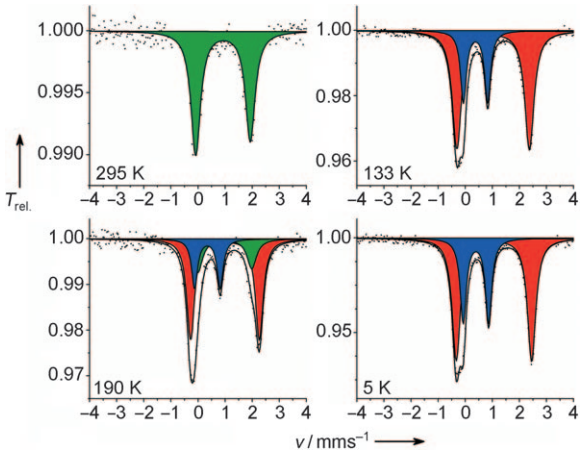

Figure 4. Zero-field ^{57}Fe Mössbauer spectra of $\mathbf{1}(BF_4)_4$ at different temperatures.

structural and susceptibility data, confirms the presence of the [HS-HS-HS-HS] species. After cooling to 133 K, a second doublet appears with an area fraction of 28.7% ($\delta = 0.38$ $mm\,s^{-1}$, $\Delta E_Q = 0.90$ $mm\,s^{-1}$, blue subspectrum), which is assigned to a single LS-Fe^{II} from the thermally induced spin transition. Concomitantly, the quadrupole splitting of the doublet for the remaining HS-Fe^{II} ion is slightly widened to 2.68 $mm\,s^{-1}$ (red subspectrum), which is most likely due to structural distortion of the grid upon SCO of one Fe^{II} center. A spectrum at intermediate temperatures (190 K) reflects the coexistence of the two forms, [HS-HS-HS-HS] and [HS-HS-HS-LS]. Below 133 K, the HS fraction continues to decrease, but no further change is observed after the relative populations have reached the ratio 65.8:34.2 at 80 K and 65.2:34.8 at 5.2 K (corresponding to circa 38% 2HS–2LS). It remains unclear at present why the second SCO step does not proceed to completion. An overview and a more detailed analysis of the Mössbauer spectra is given in the Supporting Information.

Redox properties of $\mathbf{1}^{4+}$ were investigated by cyclic voltammetry (CV) in MeCN solution. Compound $\mathbf{1}^{4+}$ undergoes four reversible oxidation processes at 0.642, 0.783, 1.257, and 1.438 V (versus SCE; 1–4 in Figure 5),[15] which are assigned to the stepwise one-electron Fe^{II}/Fe^{III} couples that finally lead to the all-ferric $\mathbf{1}^{8+}$ (Figure 1). Interestingly, the redox sequence consists of two pairs of relatively closely spaced processes (1/2 and 3/4 in Figure 5), with a much larger gap between the second and third redox couple. Comproportionation constants K_c for $\mathbf{1}^{5+}$, $\mathbf{1}^{6+}$, and $\mathbf{1}^{7+}$ were determined to be 2.42×10^2, 1.04×10^8, and 1.15×10^3, respectively, which reveals a pronounced thermodynamic stability of the di-

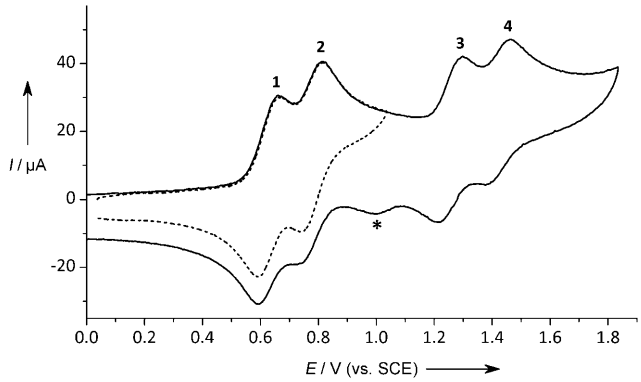

Figure 5. Cyclic voltammogram of $\mathbf{1}(BF_4)_4$ in MeCN/0.1 M NBu_4PF_6 referenced against SCE at a scan rate of 500 mV s^{-1}. —— 0.0–1.8 V, ••••• 0.04–1.0 V. The wave labeled * most likely corresponds to a decomposition product of $\mathbf{1}^{8+}$.

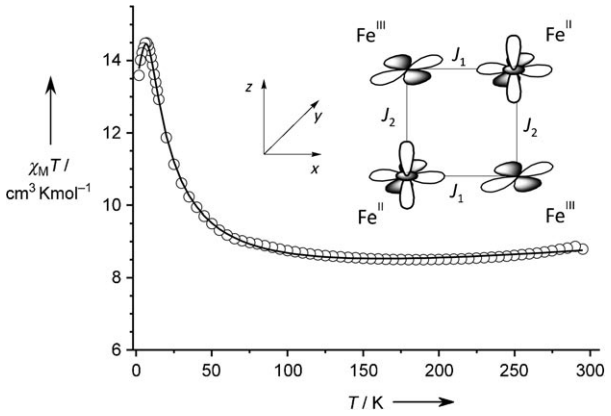

Figure 6. χT versus T plot for $\mathbf{1}(BF_4)_6$. —— best curve fit. Inset: Coupling scheme for the relevant iron d orbitals.

mixed-valence species $\mathbf{1}^{6+}$. This sequence is in accordance with the assumption that the first two oxidations occur at opposite corners of the square, where next-neighbors are still in the ferrous state (Figure 1). Compound $\mathbf{1}^{6+}$ is thus a twofold degenerate configuration. The third and fourth oxidations then occur between the already oxidized (formally) Fe^{III} centers.[16]

Given the robustness of the present tetrairon grid in various oxidation states, the di-mixed-valence species $\mathbf{1}^{6+}$ has been synthesized on a preparative scale by the addition of an excess of $AgBF_4$ to $\mathbf{1}(BF_4)_4$ in nitromethane solution at 50°. The color of the reaction mixture quickly changed from deep red to deep blue, and crystalline material of $\mathbf{1}(BF_4)_6{\cdot}3MeCN$ could be obtained by slow diffusion of diethyl ether into an acetonitrile solution of the product. The molecular structure was determined by X-ray diffraction and confirms that the $[2\times2]$ grid core has been fully retained in the doubly oxidized state (Figure 2, right). This is a rare case of a grid complex that has been structurally characterized in different oxidation states.[17] Comparison of the Fe–N bond lengths in $\mathbf{1}^{6+}$ allows two LS-Fe^{III} to be identified (Fe1/Fe1′; mean Fe–N bond length: 1.95 Å) and two HS-Fe^{II} (Fe2/Fe2′; mean Fe–N bond length: 2.20 Å) that are arranged in the anticipated diagonal fashion; that is, with equivalent sites at opposite corners of the grid. The octahedral coordination sphere for the HS-Fe^{II} is somewhat more distorted than for the LS-Fe^{III}. Because of these different metal ion characteristics, the overall grid core in the oxidized $\mathbf{1}^{6+}$ appears to be significantly more strained than in the reduced $\mathbf{1}^{4+}$ form, as the pyrazole-based ligands are severly distorted from planarity and exhibit significant twisting.

The magnetic properties of the di-mixed-valence complex $\mathbf{1}(BF_4)_6$ differ fundamentally from those of all-ferrous $\mathbf{1}(BF_4)_4$ (Figure 6). SCO behavior could not be observed for $\mathbf{1}^{6+}$. The product $\chi_M T$ remains constant over a wide temperature range (300–150 K), followed by a steep increase towards a maximum of 14.4 cm^3 K mol^{-1} at 7 K. This behavior is typical for ferromagnetically coupled systems. It was simulated using a Heisenberg-Dirac-van-Vleck Hamiltonian (HDvV; see Supporting Information) that includes terms for Zeeman and zero-field splitting.[18] The best fit was obtained when assuming two subunits [(HS-Fe^{II})-(LS-Fe^{III})] with relatively strong intrasubunit ferromagnetic coupling ($J_1 = +7.9$ cm^{-1}) and much weaker intersubunit coupling ($J_2 = +2.7$ cm^{-1}). The ferromagnetic coupling can be explained in terms of partial orthogonality of the magnetic orbitals (Figure 6, inset).[14]

The presence of two LS-Fe^{III} and two HS-Fe^{II} in $\mathbf{1}^{6+}$ was also confirmed by ^{57}Fe Mössbauer spectroscopy. The spectrum at 80 K was properly fitted by two subspectra with nearly the same area fractions (Figure 7). The sharp doublet with a

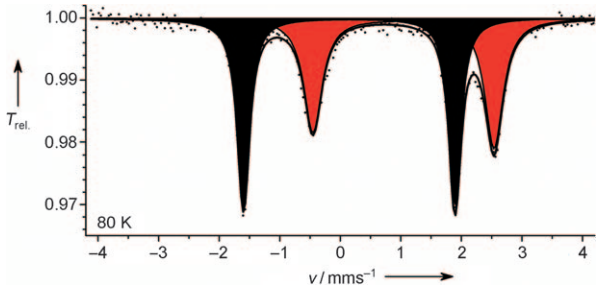

Figure 7. Zero-field ^{57}Fe Mössbauer spectrum of $\mathbf{1}(BF_4)_6$.

smaller isomeric shift and a large quadrupole splitting (black subspectrum; $\delta = 0.15$ mm s^{-1}, $\Delta E_Q = 3.49$ mm s^{-1}) corresponds to LS-Fe^{III}, whilst the broader signal at $\delta = 1.04$ mm s^{-1} stems from the HS-Fe^{II} ions (red subspectrum). The significantly larger quadrupole splitting for the HS-Fe^{II} centers ($\Delta E_Q = 2.99$ mm s^{-1}) compared to HS-Fe^{II} in the reduced $\mathbf{1}^{4+}$ case probably reflects the structural distortion of the grid core in the oxidized $\mathbf{1}^{6+}$.

UV/Vis spectra (210–2000 nm) were recorded in MeCN solution (Supporting Information, Figure S5, S6). Compound $\mathbf{1}^{4+}$ shows bands (210–400 nm) corresponding to ligand-based $\pi\rightarrow\pi^*$ transitions.[13] Additional bands found in the region from 500 to 650 nm can be deconvoluted as three overlapping absorptions that are attributed to MLCT transitions. For mixed-valent $\mathbf{1}^{6+}$, two bands (apart from the ligand-based bands) are observed at 587 and 749 nm, whilst no absorption appears in the NIR region. The relatively broad band at lowest energy (749 nm) may possibly be assigned to an

intervalence charge-transfer (IVCT) transition. A more detailed analysis of the optical and photophysical properties of $\mathbf{1}^{n+}$ is in progress.

In conclusion, a unique multistable [2×2] grid complex with two orthogonal switching modes, SCO and redox, is presented. Oxidation also switches the magnetic coupling from antiferromagnetic to ferromagnetic. The presence of twofold degenerate configurations in either the all-ferrous [HS-LS-HS-LS] form of $\mathbf{1}^{4+}$ or the mixed-valent $\mathbf{1}^{6+}$, in both cases with identical metal ions located at diagonal vertices of the grid, make these systems attractive for use as molecular components in QCA.

Received: March 14, 2010
Published online: September 13, 2010

Keywords: grid complexes · iron complexes · mixed-valent compounds · molecular switches · spin crossover

[1] a) J.-F. Létard, P. Guionneau, L. Goux-Capes, *Top. Curr. Chem.* **2004**, *235*, 221 – 249; b) O. Kahn, C. J. Martinez, *Science* **1998**, *279*, 44 – 48; c) P. Gütlich, A. Hauser, H. Spiering, *Angew. Chem.* **1994**, *106*, 2109 – 2141; *Angew. Chem. Int. Ed. Engl.* **1994**, *33*, 2024 – 2054; d) H. Toftlund, *Coord. Chem. Rev.* **1989**, *94*, 67 – 108.

[2] a) A. Bousseksou, G. Molnár, J. A. Real, K. Tanaka, *Coord. Chem. Rev.* **2007**, *251*, 1822 – 1833; b) A. B. Gaspar, M. C. Muñoz, J. A. Real, *J. Mater. Chem.* **2006**, *16*, 2522 – 2533; c) B. A. Leita, B. Mourabaki, K. S. Murray, J. P. Smith, J. D. Cashion, *Chem. Commun.* **2004**, 156 – 157; d) K. Nakano, N. Suemura, K. Yoneda, S. Kawata, S. Kaizaki, *Dalton Trans.* **2005**, 740 – 743; e) K. Yoneda, K. Adachi, S. Hayami, Y. Maeda, M. Katada, A. Fuyuhiro, S. Kawata, S. Kaizaki, *Chem. Commun.* **2006**, 45 – 47; f) J.-F. Létard, C. Carbonera, J. A. Real, S. Kawata, S. Kaizaki, *Chem. Eur. J.* **2009**, *15*, 4146 – 4155.

[3] a) K. S. Murray, C. J. Kepert, *Top. Curr. Chem.* **2004**, *233*, 195 – 228; b) K. S. Murray, *Eur. J. Inorg. Chem.* **2008**, 3101 – 3121.

[4] M. Ruben, J. Rojo, F. J. Romero-Salguero, L. H. Uppadine, J.-M. Lehn, *Angew. Chem.* **2004**, *116*, 3728 – 3747; *Angew. Chem. Int. Ed.* **2004**, *43*, 3644 – 3662.

[5] a) E. Breuning, M. Ruben, J.-M. Lehn, F. Renz, Y. Garcia, V. Ksenofontov, P. Gütlich, E. Wegelius, K. Rissanen, *Angew. Chem.* **2000**, *112*, 2563 – 2566; *Angew. Chem. Int. Ed.* **2000**, *39*, 2504 – 2507; b) M. Ruben, E. Breuning, J.-M. Lehn, V. Ksenofontov, F. Renz, P. Gütlich, G. B. M. Vaughan, *Chem. Eur. J.* **2003**, *9*, 4422 – 4429.

[6] a) M. Nihei, M. Ui, M. Yokota, L. Han, A. Maeda, H. Kishida, H. Okamoto, H. Oshio, *Angew. Chem.* **2005**, *117*, 6642 – 6645; *Angew. Chem. Int. Ed.* **2005**, *44*, 6484 – 6487; b) I. Boldog, F. J. Muñoz-Lara, A. B. Gaspar, M. C. Muñoz, M. Seredyuk, J. A. Real, *Inorg. Chem.* **2009**, *48*, 3710 – 3719.

[7] a) H. Gang, G. Dong, D. Chun-Ying, M. Hong, M. Qing-jin, *New J. Chem.* **2002**, *26*, 1371 – 1377; b) Y. Zhao, D. Guo, Y. Liu, C. He, C. Duan, *Chem. Commun.* **2008**, 5725 – 5727.

[8] A. R. Stefankiewicz, J.-M. Lehn, *Chem. Eur. J.* **2009**, *15*, 2500 – 2503.

[9] D.-Y. Wu, O. Sato, Y. Einaga, C.-Y. Duan, *Angew. Chem.* **2009**, *121*, 1503 – 1506; *Angew. Chem. Int. Ed.* **2009**, *48*, 1475 – 1478.

[10] a) I. Amlani, A. O. Orlov, G. Toth, G. H. Bernstein, C. S. Lent, G. L. Snider, *Science* **1999**, *284*, 289 – 291; b) C. S. Lent, *Science* **2000**, *288*, 1597 – 1599; c) P. J. Low, *Dalton Trans.* **2005**, 2821 – 2824.

[11] a) J. Jiao, G. J. Long, F. Grandjean, A. M. Beatty, T. P. Fehlner, *J. Am. Chem. Soc.* **2003**, *125*, 7522 – 7523; b) J. Jiao, G. J. Long, L. Rebbouh, F. Grandjean, A. M. Beatty, T. P. Fehlner, *J. Am. Chem. Soc.* **2005**, *127*, 17819 – 17831.

[12] L. N. Dawe, T. S. M. Abedin, L. K. Thompson, *Dalton Trans.* **2008**, 1661 – 1675.

[13] J. I. van der Vlugt, S. Demeshko, S. Dechert, F. Meyer, *Inorg. Chem.* **2008**, *47*, 1576 – 1585.

[14] O. Kahn, *Molecular Magnetism*, VCH, Weinheim, **1993**.

[15] The fourth redox process becomes quasi reversible at lower scan rates.

[16] a) M. Ruben, E. Breuning, M. Barboiu, J.-P. Gisselbrecht, J.-M. Lehn, *Chem. Eur. J.* **2003**, *9*, 291 – 299; b) D. M. Bassani, J.-M. Lehn, S. Serroni, F. Puntoriero, S. Campagna, *Chem. Eur. J.* **2003**, *9*, 5936 – 5946.

[17] T. Matsumoto, T. Shiga, M. Noguchi, T. Onuki, G. N. Newton, N. Hoshino, M. Nakano, H. Oshio, *Inorg. Chem.* **2010**, *49*, 368 – 370.

[18] Full-matrix diagonalization of the spin Hamiltonian for exchange coupling, zero-field splitting, and Zeeman splitting was performed with the julX program (E. Bill, Max Planck Institute for Bioinorganic Chemistry, Mülheim/Ruhr, Germany).

